Corneal Mesenchymal Stromal Cells Are Directly Antiangiogenic via PEDF and sFLT-1

Medi Eslani,[1] Ilham Putra,[1] Xiang Shen,[1] Judy Hamouie,[1] Neda Afsharkhamseh,[1] Soroush Besharat,[2] Mark I. Rosenblatt,[1] Reza Dana,[3] Peiman Hematti,[2] and Ali R. Djalilian[1]

[1]Department of Ophthalmology and Visual Sciences, University of Illinois at Chicago, Chicago, Illinois, United States
[2]Department of Medicine and University of Wisconsin Carbone Cancer Center, University of Wisconsin-Madison, School of Medicine and Public Health, Madison, Wisconsin, United States
[3]Schepens Eye Research Institute, Massachusetts Eye and Ear Infirmary, Department of Ophthalmology, Harvard Medical School, Boston, Massachusetts, United States

Correspondence: Ali R. Djalilian, Department of Ophthalmology and Visual Sciences, University of Illinois at Chicago, 1855 W. Taylor Street, EEI, 3164, Chicago, IL 60612 USA; adjalili@uic.edu.
Peiman Hematti, Department of Medicine, University of Wisconsin-Madison, School of Medicine and Public Health, 4033 WIMR, 1111 Highland Avenue, Madison, WI 53705 USA; pxh@medicine.wisc.edu.

Submitted: July 23, 2017
Accepted: September 26, 2017

Citation: Eslani M, Putra I, Shen X, et al. Corneal mesenchymal stromal cells are directly antiangiogenic via PEDF and sFLT-1. *Invest Ophthalmol Vis Sci*. 2017;58:5507–5517. DOI:10.1167/iovs.17-22680

Purpose. To evaluate the angiogenic properties of corneal derived mesenchymal stromal cells (Co-MSC).

Methods. Co-MSCs were extracted from human cadaver, and wild-type (C57BL/6J) and *SERPINF1*$^{-/-}$ mice corneas. The MSC secretome was collected in a serum-free medium. Human umbilical vein endothelial cell (HUVEC) tube formation and fibrin gel bead assay (FIBA) sprout formation were used to assess the angiogenic properties of Co-MSC secretome. Complete corneal epithelial debridement was used to induce corneal neovascularization in wild-type mice. Co-MSCs embedded in fibrin gel was applied over the debrided cornea to evaluate the angiogenic effects of Co-MSCs in vivo. Immunoprecipitation was used to remove soluble fms-like tyrosine kinase-1 (sFLT-1) and pigment epithelium-derived factor (PEDF, SERPINF1 gene) from the Co-MSC secretome.

Results. Co-MSC secretome significantly inhibited HUVECs tube and sprout formation. Co-MSCs from different donors consistently contained high levels of antiangiogenic factors including sFLT-1 and PEDF; and low levels of the angiogenic factor VEGF-A. In vivo, application of Co-MSCs to mouse corneas after injury prevented the development of corneal neovascularization. Removing PEDF or sFLT-1 from the secretome significantly diminished the antiangiogenic effects of Co-MSCs. Co-MSCs isolated from *SERPINF1*$^{-/-}$ mice had significantly reduced antiangiogenic effects compared to *SERPINF1*$^{+/+}$ (wild-type) Co-MSCs.

Conclusions. These results illustrate the direct antiangiogenic properties of Co-MSCs, the importance of sFLT-1 and PEDF, and their potential clinical application for preventing pathologic corneal neovascularization.

Keywords: cornea, mesenchymal stromal cells, sFLT-1, angiogenesis, PEDF

Mesenchymal stromal cells (MSCs) play an important role in tissue repair and maintenance and provide an attractive candidate for cell-based therapies.[1–3] Bone marrow MSCs, and to a lesser extent adipose and umbilical cord derived MSCs, have been investigated for a wide range of human diseases based on their anti-inflammatory, antifibrotic and other tissue repair properties.[4–9] We hypothesized that corneal tissue MSCs may be particularly suitable for therapeutic applications in the cornea.

Absence of blood vessels in the cornea is integral to its transparency and its immune-privileged status.[10] Corneal avascularity is largely maintained through the local production of antiangiogenic factors, including VEGF receptor 3; soluble fms-like tyrosine kinase-1 (sFLT-1; also known as soluble VEGF receptor 1); and pigment epithelium derived factor (PEDF).[11,12] Corneal neovascularization is often the final consequence of severe corneal infections or inflammation, which alter the balance in favor of angiogenic factors. Importantly, neovascularization makes the cornea less amenable to treatments via cadaveric corneal transplantation given the loss of the corneal immune privilege.[13]

In this current study, we test the hypothesis that cornea-derived MSCs have intrinsic antiangiogenic properties and further investigate the mechanism for their direct antiangiogenic effects.

Methods

Mice

All experiments in mice were conducted in compliance with the ARVO Statement for the Use of Animals in Ophthalmic and Vision Research. The protocols were approved by the Animal Care & Use Committee of the University of Illinois at Chicago (UIC). *SERPINF1*$^{-/-}$ on C57BL/6J background mice were provided by Paul J. Grippo, PhD, (UIC). C57BL/6J mice were used as wild-type.

MSC Culture

Human and mice Co-MSCs were isolated and expanded as described before.[1,2,14,15] Briefly, the corneoscleral button from

Copyright 2017 The Authors

This work is licensed under a Creative Commons Attribution-NonCommercial-NoDerivatives 4.0 International License.

Table. Antibodies Used for Flow Cytometry

Antibody	Species	Fluorochrome	Clone	Catalog Number	Manufacturer
CD90	Human	PE-Cy7	5E10	328124	BioLegend
CD39	Human	FITC	A1	328206	BioLegend
CD73	Human	BV510	AD2	563198	BD Pharmingen
CD106	Mouse	FITC	MVCAM.A	105705	BioLegend
CD45	Mouse	FITC	30-F11	103107	BioLegend
Sca1	Mouse	FITC	D7	108105	BioLegend
CD11b	Mouse	FITC	M1/70	101205	BioLegend
CD44	Mouse	FITC	IM7	103005	BioLegend
CD105	Mouse	PE	MJ7/18	120407	BioLegend
CD73	Mouse	PE	TY/11.8	127205	BioLegend
CD29	Mouse	PE	HMÖ1-1	102207	BioLegend

healthy cadaver eyes (provided by Eversight Eye Bank, Ann Arbor, MI, USA) or freshly enucleated mouse eyes were washed five times with PBS containing 2X Antibiotic-Antimycotic and 2X penicillin- streptomycin (both from Thermo Fisher Scientific, Waltham, MA, USA). After removing the central button with a trephine, the limbus was cut into three segments that were placed in 2.4 IU of protease (Dispase II; Thermo Fisher Scientific) for 1 hour at 37°C. Intact epithelial sheets were removed from stroma. The limbal segments were cut into small pieces and incubated in collagenase Type I (0.5 mg/mL) (Sigma-Aldrich Corp., St. Louis, MO, USA) in DMEM/F12 media (Thermo Fisher Scientific) overnight at 37°C or used directly for explant culture. The digests were filtered through a 70-μm nylon strainer to obtain a single-cell suspension. They were seeded onto 1% gelatin (Sigma-Aldrich Corp.)–coated wells of a 6-well tissue culture plate in alpha MEM media supplemented with 10% fetal bovine serum, 1X L-Glutamine, and 1X NEAA (all from Corning, Manassas, VA, USA). Culture media were changed every other day, and cells were subcultured by brief digestion with reagent (TrypLE Express; Thermo Fisher Scientific) when 80% confluent.

Cell Transplantation

Total limbal stem cell deficiency was induced by total corneal epithelial debridement as described before.[16] A 6-0 nylon suture was prepassed through the lids (in preparation for closing the lids afterward). Subsequently, 0.2 μL thrombin (Ethicon, Somerville, NJ, USA) was placed over the debrided cornea. A total of 5000 cells, resuspended in 3 μL fibrinogen (Ethicon), were transferred over the cornea. After the gel formed, the suture was tightened. Erythromycin ophthalmic ointment was applied. The suture was removed after 3 days.

MSC Secretome

Upon reaching 100% confluency in a T175 flask, the MSCs were washed with 30 mL prewarmed PBS 3 times. The media was then changed to phenol red free alpha MEM media supplemented with 1X L-Glutamine, and 1X NEAA. The conditioned media was collected after 48 hours. The cells were trypsinzed and counted at the same time. The conditioned media was centrifuged with 500 G speed for 15 minutes to remove any cells or debris. The supernatant was transferred to a new tube and was used for experiments or kept at 4°C for up to a week.

Tube Formation Assay

Human umbilical vein endothelial cells (HUVEC; Thermo Fisher Scientific) were cultivated in specialty media (Medium 200; Thermo Fisher Scientific) fortified with low serum growth supplement (LSGS). At passage 4, the cells were detached and resuspended in medium (Thermo Fisher Scientific) + 10% LSGS, which was used as the base media. The 96-well plate were filled with 75 μL gelatinous protein mixture (Matrigel; Thermo Fisher Scientific) and allowed to solidify at 37°C, after which HUVECs (2×10^4 cells/75 μL) were gently seeded on top of the gel. Subsequently, 75 μL of secretome, complete media, or specialty media (Thermo Fisher Scientific) was added as the testing condition, positive, and negative controls, respectively. After 6 hours, network structures were analyzed and photographed at ×4 magnification (Leica Microsystems, Wetzlar, Germany). Total tubule length per image was calculated using angiogenesis analyzer plugin of ImageJ (http://imagej.nih.gov/ij/; provided in the public domain by the National Institutes of Health [NIH], Bethesda, MD, USA).

Fibrin Induced Bead Assay

Fibrin induced bead assay (FIBA) was performed as described previously.[17] Briefly, HUVECs (passage 3 to 5) were stained with red dye (Cat. No. C34565, CellTracker Deep Red Dye Thermo Fisher). A total of 2500 presterilized microcarrier beads (Cytodex 3; Sigma-Aldrich Corp., Cat. No. C3275) were mixed with 1×10^6 HUVECs in specialty medium (Thermo Fisher Scientific) + LSGS (complete media) and incubated overnight. A total of 250 precoated beads in 500 μL of 2 mg/mL fibrinogen (Cat. No. F8630; Sigma-Aldrich Corp.) + 0.15 units/mL aprotinin (Cat. No. A6106; Sigma-Aldrich Corp.) was seeded per well of a 24-well plate. The bead-fibrinogen solution was coagulated by adding 0.625 unit/mL thrombin (Cat. No. T7513; Sigma-Aldrich Corp.). Subsequently, 500 μL of specialty medium (Thermo Fisher Scientific) + 10% LSGS was added to the surface of the clotted fibrin gel dropwise, followed by 500 μL of secretome, complete media, or specialty medium (Thermo Fisher Scientific) as testing condition, positive, and negative controls, respectively. After 3 days, images were captured and analyzed using ImageJ software.

Immunostaining

Corneal whole mount immunostaining was done as described before.[18] Briefly, after enucleation of the eye, the cornea was dissected using a spring scissor. It was then fixed with 4% paraformaldehyde at 4°C overnight. After washing with PBS, it was incubated with 20 μg/mL serine protease (Proteinase-K; Sigma-Aldrich Corp.) for 5 minutes at room temperature followed by 100% methanol for another 30 minutes. It was then incubated with 10% serum and 2% bovine serum albumin (BSA) at 4°C overnight. Purified anti-mouse CD31 (Cat. No. 102401; BioLegend) was used as primary antibody and Rhodamine-conjugated donkey anti-rat IgG (Cat. No. 712–02–153; Jackson ImmunoResearch, West Grove, PA, USA) as

Investigative Ophthalmology & Visual Science

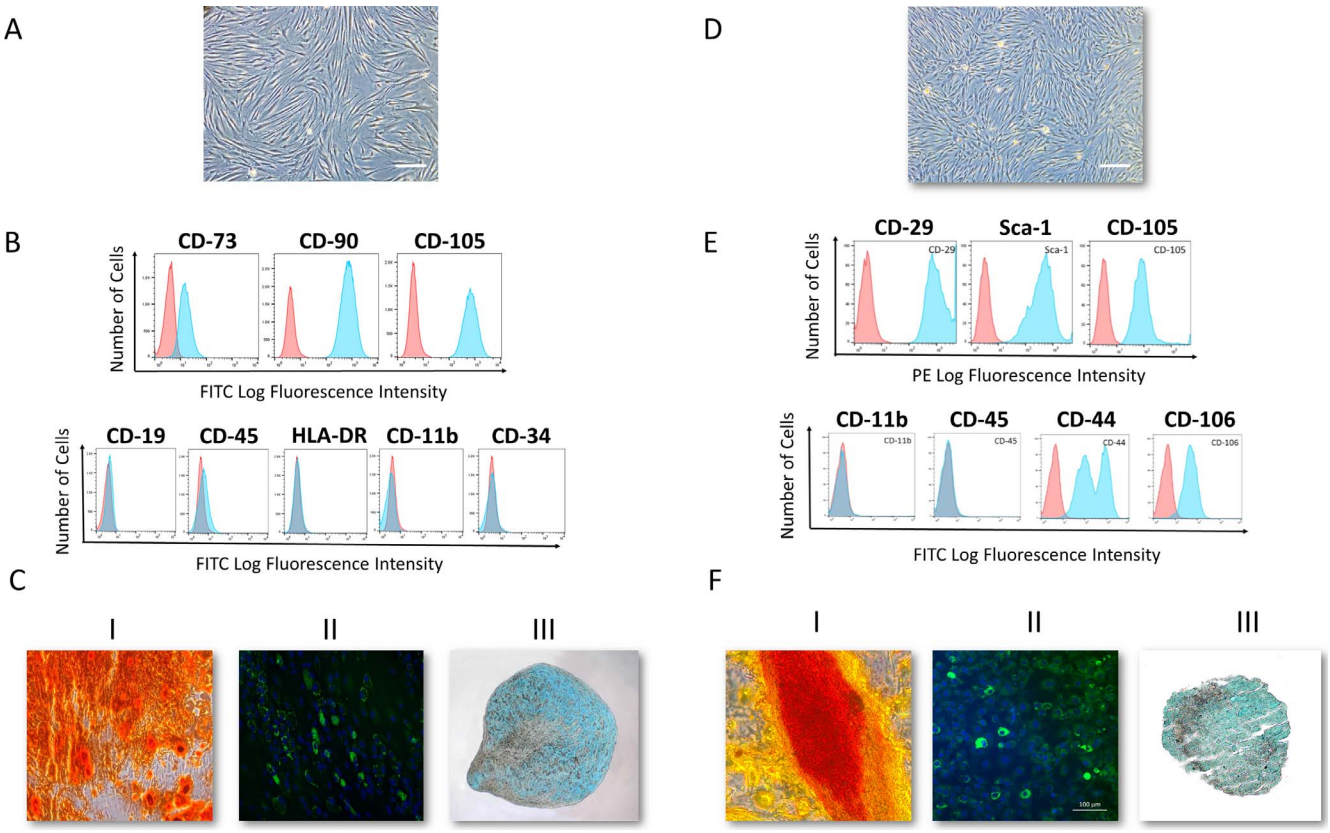

Figure 1. Human and mouse corneal stromal cells demonstrate mesenchymal stromal cells (MSC) features. (**A**) Bright-field image of passage-4 human corneal MSCs. (**B**) Flow cytometry analysis demonstrated a homogenous MSC population. More than 95% of the cells were positive for cell surface markers CD73, CD90, CD105, and negative for CD19, CD45, HLA-DR, CD11b, and CD34 ($n = 10$). (**C**) Differentiation into the three mesenchymal lineages: I: Osteogenesis: calcium deposition stained with Alizarin Red; II: Adipogenesis: lipid formation stained with LipidTOX; III: Chondrogenesis: Glycosaminoglycans stained with Alcian Blue. (**D**) Bright-field microscopy image of passage-4 mouse corneal MSCs. (**E**) Flow cytometry analysis demonstrated a homogenous MSC population. More than 95% of the cells are positive for cell surface markers CD29, Sca-1, CD105, CD44 and CD106 and negative for CD11b, and CD45. (**F**) Differentiation into the three mesenchymal lineages: I: Calcium deposition stained with Alizarin Red; II: Lipid formation stained with LipidTOX; III: Glycosaminoglycans stained with Alcian Blue.

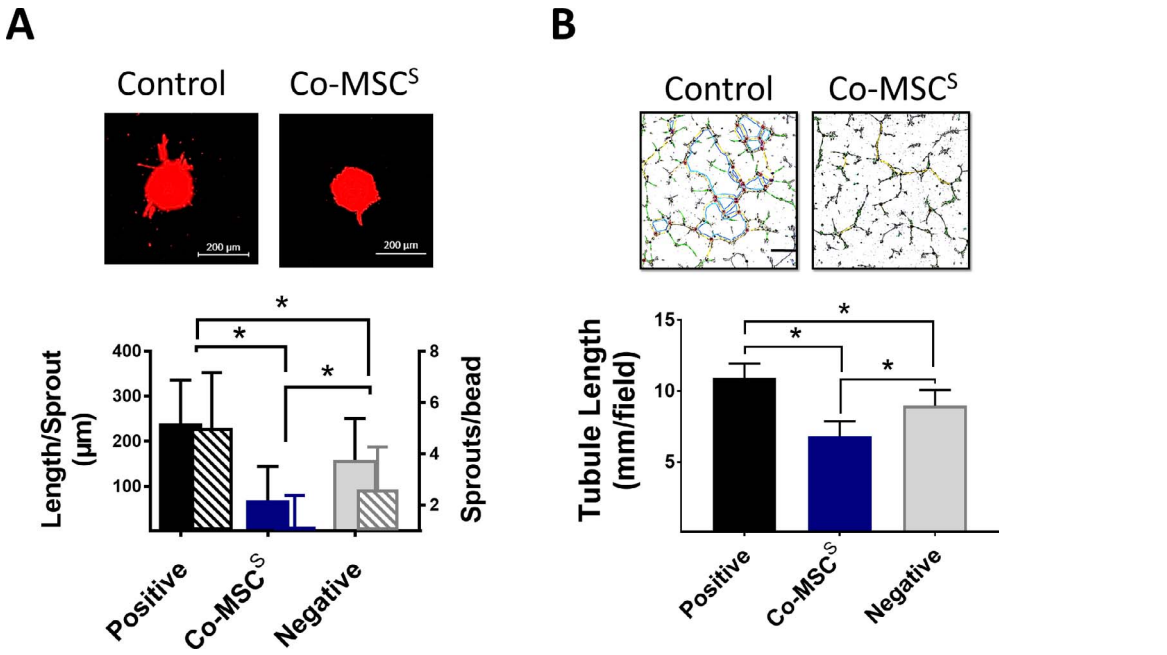

Figure 2. Corneal MSCs (Co-MSCs) are directly antiangiogenic in vitro. (**A**) Co-MSC secretome significantly inhibited mean sprout count per bead and mean sprout length in a fibrin-induced bead assay ($n = 5$). *$P < 0.001$. *Scale bars*: 200 µm. (**B**) Co-MSC secretome (6.8 ± 1.0 mm/field) significantly reduced tubule formation in a HUVEC assay ($n = 5$). *$P < 0.003$. The values shown are mean ± SD (*error bars*). ^{S}, secretome.

Investigative Ophthalmology & Visual Science

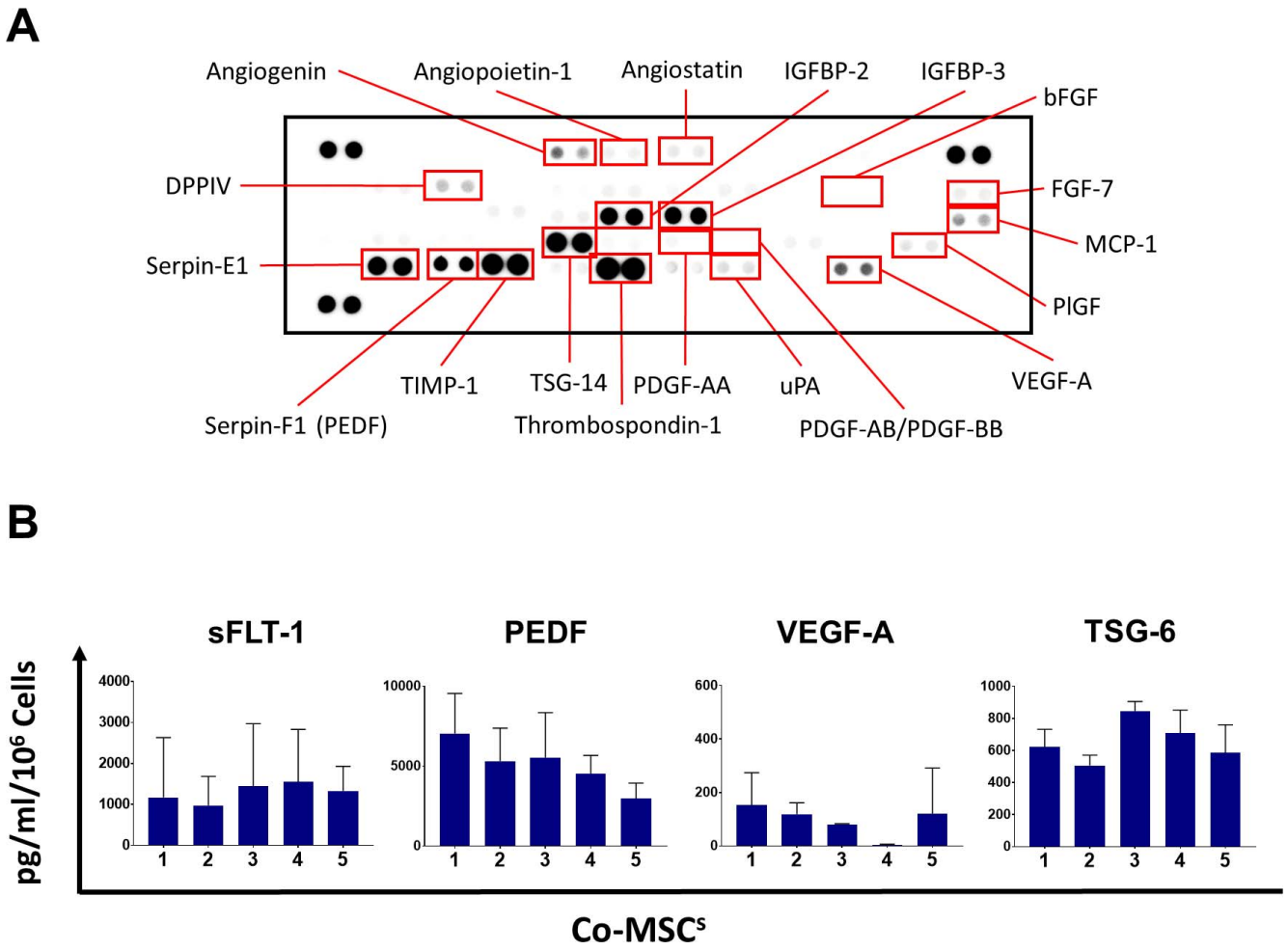

Figure 3. Co-MSCs have an antiangiogenic profile by protein expression. (**A**) Human angiogenesis array was used to profile pro- and antiangiogenesis mediators in the Co-MSC secretome. It revealed it has high levels of antiangiogenic factors, whereas low levels of proangiogenic factors. (**B**) The secretome from Co-MSCs contains high levels of sFLT-1 (1875 ± 677 pg/mL); PEDF (4829 ± 2342 pg/mL); TSG-6 (643.3 ± 149.1 pg/mL); and low amount of VEGF-A (106.9 ±103.3 pg/mL; $n = 5$). The values shown are mean ± SD (*error bars*).

secondary antibody. The slides were visualized and photographed using a commercial microscope (Zeiss LSM 710; Carl Zeiss Meditec, Jena, Germany). To make the quantification more objective, we used VesselJ[19] to quantify the ratio of vascularized area to total corneal area.

Human Proteome Array Analysis

The expression levels of proteins known for their roles in angiogenesis were analyzed using an antibody array (Proteome Profiler Human Angiogenesis Array Kit; R&D System, Minneapolis, MN, USA) according to the manufacturer's instruction.

Enzyme-Linked Immunosorbent Assay

Human PEDF (Cat. No. DY1177-05); sFLT-1 (Cat. No. DVR100B); and VEGF-A (Cat. No. DVE00) proteins were detected with commercially available ELISA kits (all from R&D Systems) according to the manufacturer's protocol. The obtained values were normalized to total cell numbers.

Immunoprecipitation (IP)

Co-MSC secretome was incubated with 25 µg/mL anti-PEDF (Cat. No. AF1177); anti-sFlt1 (Cat. No. AF321); or normal Goat IgG (Cat. No. AB 108-C) antibody (all from R&D) at 4°C overnight. After washing of the beads with IP buffer (Cat. No. I-5779; Sigma-Aldrich Corp.), samples were incubated with 30 µl of protein G beads (Sigma-Aldrich Corp. Cat. No. P-3296) at 4° C for 2 hours. The samples were centrifuged at 12000 g for 30 seconds. The supernatant was checked for the efficiency of IP. It was then used for the experiments.

siRNA Transfection

After reaching 70% to 80% of confluency, Co-MSCs were transfected with 50 nM *SERPINF1* siRNA (Cat. No. sc-40947; Santa Cruz Biotechnology, Dallas, TX, USA) or scrambled siRNA (Cat. No. D-001205; Dharmacon, Lafayette, CO, USA) in TransIT-TKO siRNA transfection reagent (Cat. No. MIR2150; Mirus Bio LLC, Madison, WI, USA). The transfection efficiency was tested with ELISA on the secretome.

Flow Cytometry

The cells were detached as described above. They were incubated with Fc block (Cat. No. 564220 for human; BD Pharmingen, San Jose, CA, USA, and TruStain fcX [anti-mouse CD16/32], Cat. No. 101319 for mouse; BioLegend) and stained at 4°C for 20 minutes in antibody diluent (PBS with 2% FBS) with cell surface antibodies (Table). For intracellular staining, fixation buffer (Cat. No. 420801; BioLegend) and intracellular

Investigative Ophthalmology & Visual Science

staining perm wash buffer (Cat. No. 421002; BioLegend) were used according to manufacturer's protocol. Flow cytometry data was acquired on the BD LSR Fortessa (BD Pharmingen). Data were analyzed using analytical software (FlowJo; FlowJo LLC, Ashland, OR, USA).

Western Blot Analysis

Cells cultured on 100-mm dishes were rinsed twice with PBS and harvested in SDS RIPA buffer (Sigma-Aldrich Corp.) supplemented with protease/phosphatase inhibitors (Sigma-Aldrich Corp.). After protein concentration measurement, equal amounts of each sample were mixed with 2X Laemmli buffer (Bio-Rad Laboratories, Hercules, CA, USA) and 5% beta-mercaptoethanol (Sigma-Aldrich Corp.), denatured by heating at 95°C for 10 minutes, and subjected to electrophoresis on 4% to 20% Tris-Glycine gels (Invitrogen, Grand Island, NY, USA). The protein bands were transferred to polyvinylidene difluoride membranes. The membranes were incubated in 5% BSA in tris-buffered saline (TBS) for 1 hour followed by an overnight incubation (4°C) with primary antibodies at the optimal concentration. The membranes were washed with TBS with 0.03% Tween 20 and incubated with the horseradish peroxidase–conjugated secondary antibody for 1 hour at room temperature. Detection was performed with commercial detection system (ECL Plus Western Blotting Detection System; Amersham, Buckinghamshire, UK). Mouse Serpin F1/PEDF antibody (AF1149) was purchased from R&D Systems.

Data Analysis and Statistical Comparisons

To obviate observer bias and to increase reproducibility, all the animal surgeries were done by one of the authors who was blinded to the treatment arms. Data collection and analyses were done in a masked fashion to minimize inter- and intraobserver bias. Eyes with infection were excluded from the study. Corneal infection was defined as corneal edema, hypopyon, and exudate within the first 7 days after the procedure. Results are presented as the mean ± SD of three independent experiments. Normality of the data was tested using D'Agostino & Pearson normality test. Based on normality test, Mann-Whitney *U*-test or 2-sided student's *t*-test was performed to determine significance, which was set at $P < 0.05$. For more than two arms comparison, 1-way ANOVA with Tukey's post hoc correction was used. All statistics were performed using statistical and spreadsheet software (GraphPad Prism 7.0; GraphPad Software, Inc., La Jolla, CA, USA, and Excel; Microsoft Corp., Redmond, WA, USA).

Results

Co-MSC Secretome Is Antiangiogenic

Co-MSCs were successfully isolated from human and mouse corneas and characterized to meet the minimal International Society of Cell Therapy criteria for defining MSCs (Fig. 1). Previous studies have demonstrated that the therapeutic effects of MSCs are largely mediated through their secreted factors.[20,21] We proceeded to test Co-MSC secretome using in vitro assays of angiogenesis. The results indicated that Co-MSC secretome significantly inhibits vascular sprouting and endothelial tube formation compared to control media (Figs. 2A, 2B).

Co-MSCs Have an Antiangiogenic Profile by Protein Expression

Human angiogenesis array was used to profile pro- and antiangiogenesis mediators in the Co-MSC secretome. It revealed it has high levels of antiangiogenic factors, whereas low levels of proangiogenic factors (Fig. 3A). Based on the results of proteome array and previous studies, we focused specifically on sFLT-1 and PEDF (product of gene serine proteases inhibitor F1; *SERPINF1*), two important soluble mediators of corneal angiogenic privilege.[11,22,23] Co-MSCs from multiple donors consistently expressed and secreted high levels of sFLT-1 and PEDF, whereas Co-MSCs secretome from multiple donors contained low levels of VEGF-A. Co-MSCs also secreted high levels of TNF-stimulated gene 6 (TSG 6), a well-known anti-inflammatory mediator of MSCs (Fig. 3B).

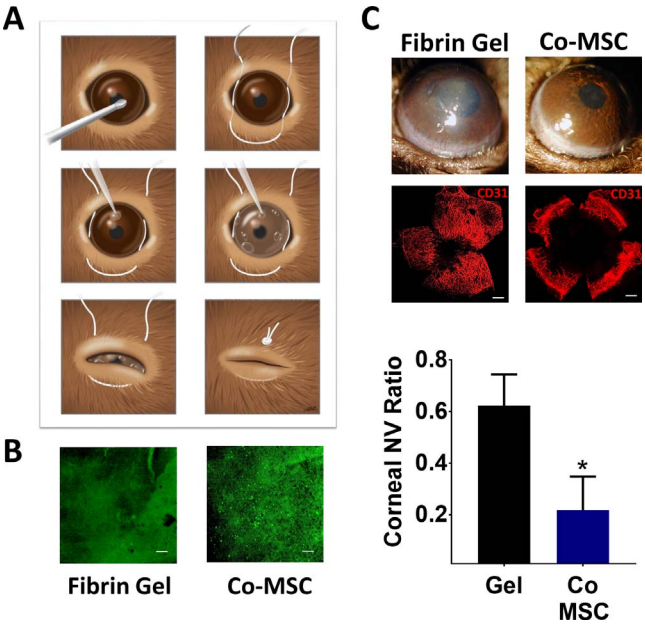

Figure 4. Co-MSCs inhibit pathologic corneal neovascularization in vivo. (**A**) Schematic illustration shows the steps for debriding the epithelium, MSC delivery using fibrin gel and temporarily closing the lids. (**B**) In vivo microscopy confirmed the presence of fluorescent-labeled MSCs in the cornea three days after the procedure. *Scale bars*: 200 μm. (**C**) The slit lamp photos and CD31 staining demonstrated both Co-MSCs significantly prevented corneal neovascularization compared to fibrin gel alone 14 days after injury. The values shown are mean ± SD (*error bars*). $^*P < 0.001$. We used 1-way ANOVA and then 2-sided *t*-test were used to compare the groups ($n = 5$).

Co-MSCs Have Antiangiogenic Effects In Vivo

We tested Co-MSCs in an in vivo model of pathologic corneal neovascularization. In this model, the entire corneal epithelium is mechanically debrided that results in severe corneal neovascularization. MSCs were embedded in a fibrin gel and applied to the cornea immediately after the injury (Fig. 4A). In vivo microscopy confirmed the presence of fluorescent-labeled MSCs in the cornea 3 days after the procedure (Fig. 4B). The results demonstrated that Co-MSCs could effectively prevent corneal neovascularization (Fig. 4C).

Antiangiogenic Effects of Co-MSCs Depend on Secreted sFLT-1 and PEDF

To investigate the role of sFLT-1 and PEDF in the antiangiogenic effects of Co-MSCs, immunoprecipitation was used to remove them from the secretome. Removing sFLT-1 or PEDF from Co-MSC secretome resulted in a significantly increased tubule formation in a HUVEC assay. The effects appeared to be

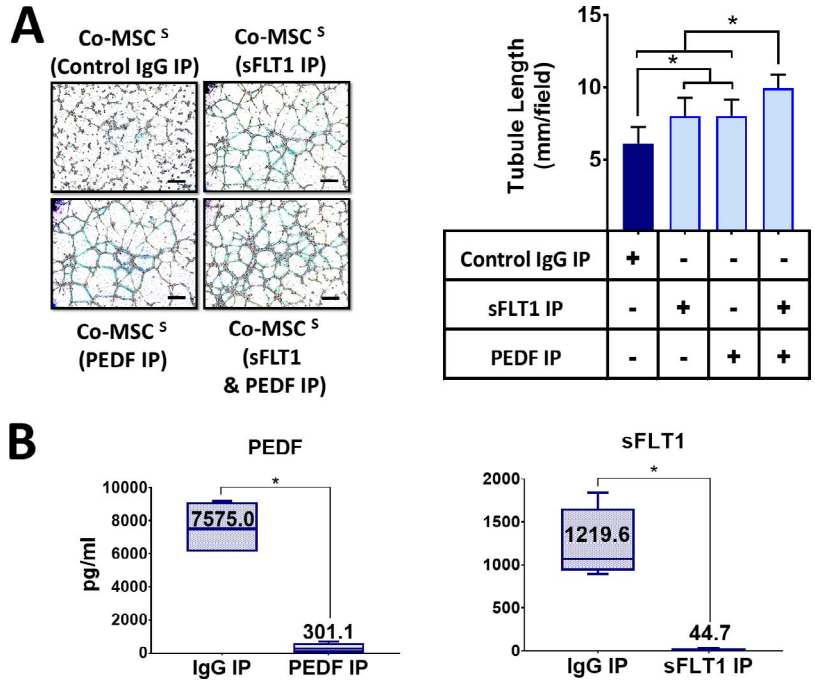

Figure 5. Direct antiangiogenic properties of Co-MSCs depend on PEDF and sFLT-1. (**A**) Removing sFLT-1 and PEDF with neutralizing antibody capturing and immunoprecipitation abrogated the antiangiogenic property of Co-MSC secretome in a HUVEC assay ($n = 5$ 1-way ANOVA and then 2-sided *t*-test were used to compare the groups). $^*P < 0.001$. (**B**) The efficiency of immunoprecipitation for PEDF and sFLT1 was more than 95% determined by ELISA ($n = 5$, 2-sided *t*-test: $^*P < 0.0001$). *Boxes* show the interquartile (25%–75%) range; *whiskers* encompass the range (minimum–maximum); and *horizontal* lines represent the mean. *Scale bars*: 100 µm. IP, immunoprecipitation.

additive; removing both factors resulted in a more significant reduction in the antiangiogenic effects of Co-MSC secretome (Fig. 5A). The efficiency of immunoprecipitation for PEDF and sFLT1 was more than 95% as determined by ELISA (Fig. 5B). Knocking down PEDF in Co-MSCs, using siRNA, likewise decreased the antiangiogenic activity of its secretome in vitro (Fig. 6). To examine the effect of PEDF in vivo, we isolated Co-mMSCs from *SERPINF1*$^{-/-}$ mice and compared them to wild-

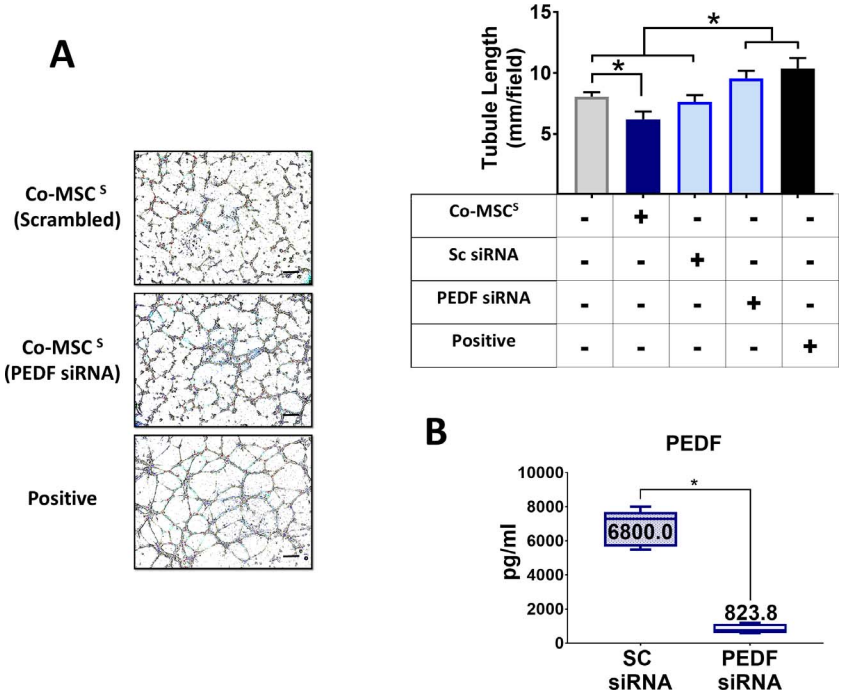

Figure 6. Direct antiangiogenic properties of Co-MSCs are in part due to PEDF. Knocking down PEDF in Co-MSCs by siRNA obviates the antiangiogenic effects of their secretome and increases tubule formation in a HUVEC assay ($n = 4$, 1-way ANOVA, and then 2-sided *t*-test were used to compare the groups). $^*P < 0.001$. (**B**) Knocking down PEDF by siRNA decreased PEDF protein by almost 90% compared to scrambled siRNA ($n = 4$, 2-sided *t*-test: $^*P < 0.0001$). *Boxes* show the interquartile (25%–75%) range; *whiskers* encompass the range (minimum–maximum); and *horizontal lines* represent the mean. *Scale bars*: 100 µm. SC, Scrambled.

Investigative Ophthalmology & Visual Science

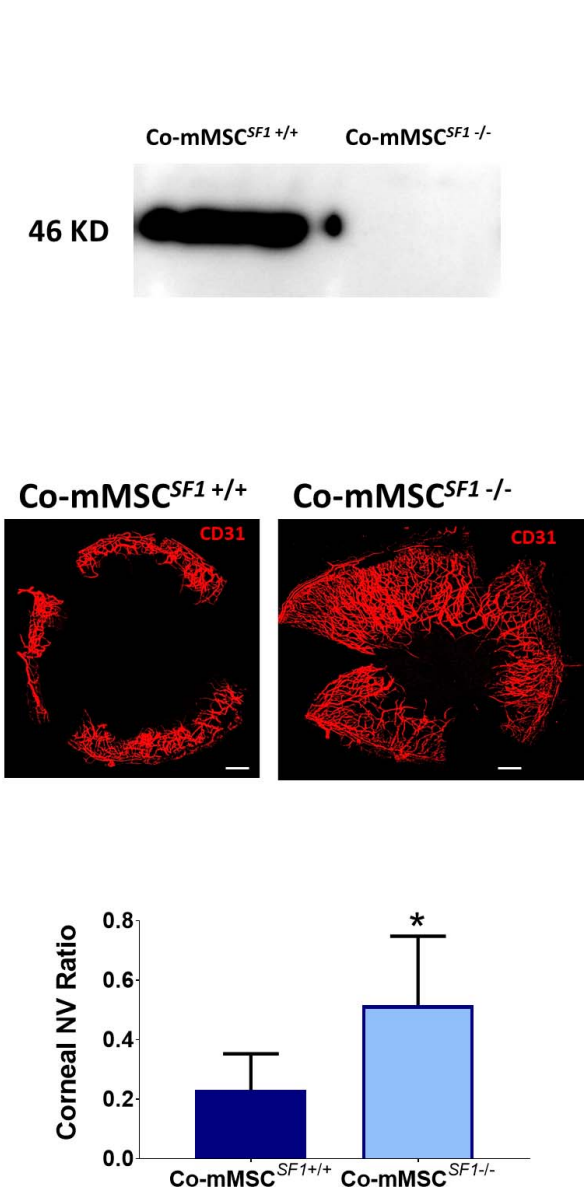

Figure 7. PEDF plays a key role on the antiangiogenic properties of Co-MSCs in vivo. (**A**) Western blot shows Co-MSCs isolated from SERPINF1$^{-/-}$ mice do not express PEDF. (**B**) Co-MSCs isolated from SERPINF1$^{-/-}$ mice had lower antiangiogenic effects, compared to wild-type (SERPINF1$^{+/+}$) Co-MSCs, when placed in fibrin gels after corneal epithelial injury in wild-type mice (same model as in Fig. 4A; $n = 5$, 2-sided *t*-test: $^{*}P = 0.0001$). *Scale bars*: 500 µm. The values shown are mean ± SD (*error bars*). Co-mMSC^{SF1}, corneal mouse MSCSERPINF1; NV, neovascularization.

type Co-mMSCs using the injury model described earlier. The results demonstrated that wild-type mouse corneas treated with *SERPINF1*$^{-/-}$ Co-mMSCs had significantly more neovascularization compared to corneas treated with wild-type Co-mMSCs (Fig. 7).

Discussion

It is well accepted that the therapeutic effects of MSCs in many disease processes are mediated largely through their immunomodulatory and anti-inflammatory properties.[21,24–26] They have been shown to modulate both innate and adaptive immune mechanisms.[27–29] Local tissue derived MSCs, which share many features with other MSCs, can have additional special attributes that may be potentially useful for certain clinical applications.[30–32] For instance, Co-MSCs were shown to have antifibrotic effects and prevent the development of corneal scarring after injury.[1]

While majority of studies have shown BM and adipose derived MSCs are proangiogenic, there has been reports that BM-MSCs can block corneal neovascularization.[33–38] In particular, MSCs from different sources have been shown to secrete several angiostatic factors, including thrombospondin 1; tissue metalloproteinase inhibitor 1; pentraxin-3 (TSG-14); and PEDF.[37,39–47] In general, the mechanisms that have been proposed for the antiangiogenic effects of MSCs are indirectly based on their anti-inflammatory properties rather than direct antiangiogenic effects.[37] The current study provides the first direct evidence that Co-MSCs have direct antiangiogenic effects, through high secretion of antiangiogenic factors such as sFLT-1 and PEDF and low secretion of angiogenic factors including VEFG-A (Fig. 8). This finding has important translational implications for corneal diseases that involve neovascularization.

Soluble VEGF receptor (VEGFR-l, sFLT-1) predominantly derives from alternative splicing,[48] but possibly also from proteolytic cleavage of full-length VEGFR-1.[49] The molecular mechanisms of the purported antiangiogenic effects of sFLT-1 are believed to include: sequestration of VEGF ligands, much like VEGFR-1 does, and effectively reducing VEGF-mediated activation of proangiogenic receptors,[11,50] and heterodimerization with full-length VEGFR monomers to render the receptor dimer inactive, because sFLT-1 lacks the intracellular tyrosine kinase domain needed to transphosphorylate its full-length partner.[51–53] Moreover, several biologic functions of sFLT-1 have been deduced from its capacity to neutralize VEGF: antiangiogenesis, by dampening angiogenic VEGF-VEGFR-2 signaling[54,55]; anti-edema, by interfering with VEGF-mediated vascular permeability through VEGFR-1 or VEGFR-2[55,56]; and anti-inflammation, by attenuating VEGF-VEGFR-1-dependent monocyte and macrophage activation and migration.[57]

It is well accepted that sFLT-1 is an important factor in corneal avascularity.[58–61] It is produced mainly by corneal epithelial cells.[11] In our in vivo studies, the contribution of epithelial secreted sFLT-1 was not specifically studied; however, our in vitro results confirm that Co-MSCs secrete sFLT-1 at high enough level to inhibit angiogenesis.

PEDF is a 50 kD multifunctional secreted glycoprotein.[62] Many studies have substantiated its potent antiangiogenic activity and the opposing actions of PEDF and VEGF in controlling quiescence and permeability of the vasculature.[62–65] PEDF has several different mechanisms including competitive binding to the VEGFR-2,[66] γ-secretase-mediated cleavage, and translocation of a fragment of the VEGFR-1,[49,65] as well as alteration of the phosphorylation status of VEGFR-l.[49,65] The importance of PEDF in corneal avascularity has been well documented.[67–74]

This study further highlights the distinct characteristics as well as the translational potential of local tissue–derived MSCs. While MSCs from various tissues share the minimal International Society of Cell Therapy criteria for defining MSCs, they often have differences in functional properties based on their tissue of origin.[75,76] In the case of Co-MSCs, while many of their anti-inflammatory effects may be potentially shared by other MSC types based on their common repertoire of anti-inflammatory factors, their direct antiangiogenic effects may be a more distinctive feature. Given the feasibility of generating clinical grade Co-MSCs from human cadaveric corneas, they provide an attractive cell source for developing regenerative

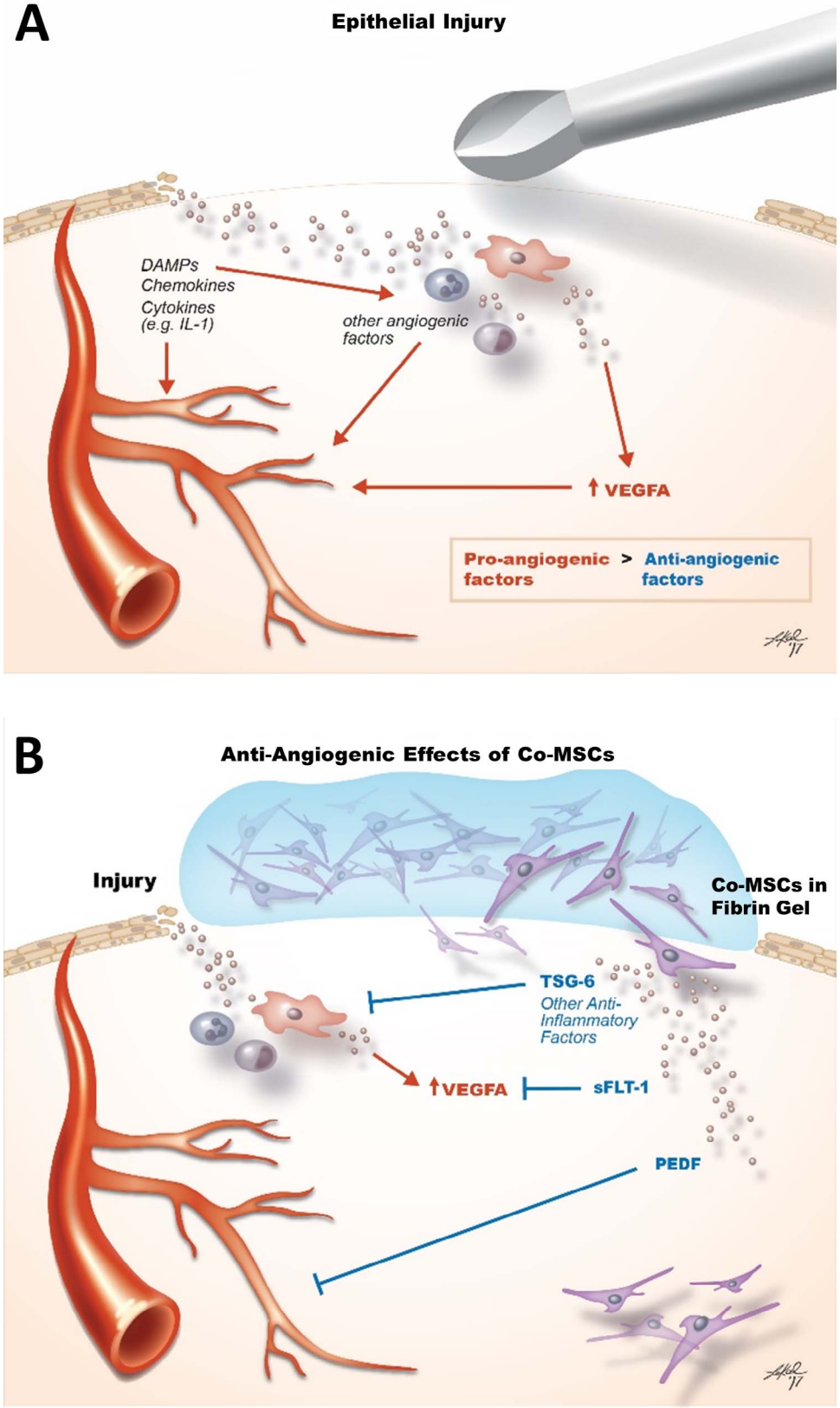

Figure 8. Schematic illustration summarizes the mechanisms by which Co-MSCs confer their antiangiogenic properties. (**A**) After corneal epithelial injury, DAMPS, chemokines, and cytokines released by the injured and resident cells directly induce angiogenesis while also recruiting inflammatory cells that further promote angiogenesis. The net effect is shifting the antiangiogenic balance of the cornea toward angiogenesis. (**B**) Co-MSCs applied to the cornea after injury modulate neovascularization directly through the secretion of antiangiogenic factors including PEDF and sFLT-1 and indirectly by suppressing inflammation via TSG6 and other anti-inflammatory factors. DAMP, damage-associated molecular pattern.

Investigative Ophthalmology & Visual Science

antiangiogenic and immunomodulatory therapies for the cornea and potentially other tissues.

Acknowledgments

The authors thank Lauren Kalinoski for assistance in creating the schematics, Ruth Zelkha for assistance with imaging, and Tara Nguyen for assistance with animal work. The authors also thank Dimitri Azar, MD MBA, Luisa DiPietro, DDS, PhD, Kyu-Yeon Han, PhD, and Hongyu Ying, PhD, at University of Illinois at Chicago for helpful scientific discussions and comments.

Supported by Clinical Scientist Development Program Award K12EY021475 (ME); R01 EY024349 (ARD); and Core Grant for Vision Research P30 EY001792 from NEI/NIH; MR130543 (ARD) from the United States Department of Defense, United States Army, Vision for Tomorrow (ARD); University of Wisconsin Carbone Cancer Center Support Grant P30 CA014520 (PH); unrestricted grant to the department from Research to Prevent Blindness; Eversight (providing both seed funding and human corneal research tissue); and UW-Madison Don Anderson fund for GVHD research. The authors alone are responsible for the content and writing of the paper.

Disclosure: **M. Eslani**, None; **I. Putra**, None; **X. Shen**, None; **J. Hamouie**, None; **N. Afsharkhamseh**, None; **S. Besharat**, None; **M.I. Rosenblatt**, None; **R. Dana**, None; **P. Hematti**, None; **A.R. Djalilian**, None

References

1. Basu S, Hertsenberg AJ, Funderburgh ML, et al. Human limbal biopsy-derived stromal stem cells prevent corneal scarring. *Sci Transl Med*. 2014;6:266ra172.
2. Mittal SK, Omoto M, Amouzegar A, et al. Restoration of corneal transparency by mesenchymal stem cells. *Stem cell reports*. 2016;7:583–590.
3. Amouzegar A, Mittal SK, Sahu A, Sahu SK, Chauhan SK. Mesenchymal stem cells modulate differentiation of myeloid progenitor cells during inflammation. *Stem cells*. 2017;35: 1532–1541.
4. Prockop DJ. Repair of tissues by adult stem/progenitor cells (MSCs): controversies, myths, and changing paradigms. *Mol Ther*. 2009;17:939–946.
5. Premer C, Blum A, Bellio MA, et al. Allogeneic mesenchymal stem cells restore endothelial function in heart failure by stimulating endothelial progenitor cells. *EBioMedicine*. 2015; 2:467–475.
6. Prockop DJ. The exciting prospects of new therapies with mesenchymal stromal cells. *Cytotherapy*. 2017;19:1–8.
7. Hatzistergos KE, Hare JM. Cell therapy: targeting endogenous repair versus remuscularization. *Circulation Res*. 2015;117: 659–661.
8. Maria AT, Toupet K, Maumus M, et al. Human adipose mesenchymal stem cells as potent anti-fibrosis therapy for systemic sclerosis. *J Autoimmunity*. 2016;70:31–39.
9. Li C, Zhen G, Chai Y, et al. RhoA determines lineage fate of mesenchymal stem cells by modulating CTGF-VEGF complex in extracellular matrix. *Nat Commun*. 2016;7:11455.
10. Perez VL, Caspi RR. Immune mechanisms in inflammatory and degenerative eye disease. *Trends in immunology*. 2015; 36:354–363.
11. Ambati BK, Nozaki M, Singh N, et al. Corneal avascularity is due to soluble VEGF receptor-1. *Nature*. 2006;443:993–997.
12. Cursiefen C, Chen L, Saint-Geniez M, et al. Nonvascular VEGF receptor 3 expression by corneal epithelium maintains avascularity and vision. *Proc Natl Acad Sci U S A*. 2006;103: 11405–11410.
13. Clements JL, Dana R. Inflammatory corneal neovascularization: etiopathogenesis. *Semin Ophthalmol*. 2011;26:235–245.
14. Byun YS, Tibrewal S, Kim E, et al. Keratocytes derived from spheroid culture of corneal stromal cells resemble tissue resident keratocytes. *PLoS One*. 2014;9:e112781.
15. Polisetty N, Fatima A, Madhira SL, Sangwan VS, Vemuganti GK. Mesenchymal cells from limbal stroma of human eye. *Mol Vis*. 2008;14:431–442.
16. Afsharkhamseh N, Movahedan A, Gidfar S, et al. Stability of limbal stem cell deficiency after mechanical and thermal injuries in mice. *Exp Eye Res*. 2016;145:88–92.
17. Nakatsu MN, Davis J, Hughes CC. Optimized fibrin gel bead assay for the study of angiogenesis. *J Vis Exp*. 2007;186.
18. Cao R, Lim S, Ji H, et al. Mouse corneal lymphangiogenesis model. *Nat Protoc*. 2011;6:817–826.
19. Rabiolo A, Bignami F, Rama P, Ferrari G. VesselJ: a new tool for semiautomatic measurement of corneal neovascularization. *Invest Ophthalmol*. Vis Sci 2015;56:8199–8206.
20. Uccelli A, de Rosbo NK. The immunomodulatory function of mesenchymal stem cells: mode of action and pathways. *Ann N Y Acad Sci*. 2015;1351:114–126.
21. Coulson-Thomas VJ, Coulson-Thomas YM, Gesteira TF, Kao WW. Extrinsic and intrinsic mechanisms by which mesenchymal stem cells suppress the immune system. *Ocul Surf*. 2016; 14:121–134.
22. Wietecha MS, Krol MJ, Michalczyk ER, Chen L, Gettins PG, DiPietro LA. Pigment epithelium-derived factor as a multifunctional regulator of wound healing. *Am J Physiol Heart Circ Physio*l. 2015;309:H812–H826.
23. Zamiri P, Masli S, Streilein JW, Taylor AW. Pigment epithelial growth factor suppresses inflammation by modulating macrophage activation. *Invest Ophthalmol Vis Sci*. 2006;47: 3912–3918.
24. Kao WW, Coulson-Thomas VJ. Cell therapy of corneal diseases. *Cornea*. 2016;35(suppl 1):S9–S19.
25. Forrester JV, Steptoe RJ, Klaska IP, et al. Cell-based therapies for ocular inflammation. *Prog Retin Eye Res*. 2013;35:82–101.
26. Choi H, Lee RH, Bazhanov N, Oh JY, Prockop DJ. Anti-inflammatory protein TSG-6 secreted by activated MSCs attenuates zymosan-induced mouse peritonitis by decreasing TLR2/NF-kappaB signaling in resident macrophages. *Blood*. 2011;118:330–338.
27. Stagg J, Galipeau J. Mechanisms of immune modulation by mesenchymal stromal cells and clinical translation. *Curr Mol Med*. 2013;13:856–867.
28. Ko JH, Lee HJ, Jeong HJ, et al. Mesenchymal stem/stromal cells precondition lung monocytes/macrophages to produce tolerance against allo- and autoimmunity in the eye. *Proc Natl Acad Sci U S A*. 2016;113:158–163.
29. Espagnolle N, Balguerie A, Arnaud E, Sensebe L, Varin A. CD54-Mediated Interaction with Pro-inflammatory Macrophages Increases the Immunosuppressive Function of Human Mesenchymal Stromal Cells. *Stem cell reports*. 2017;8:961–976.
30. Kellner J, Sivajothi S, McNiece I. Differential properties of human stromal cells from bone marrow, adipose, liver and cardiac tissues. *Cytotherapy*. 2015;17:1514–1523.
31. Klimczak A, Kozlowska U. Mesenchymal stromal cells and tissue-specific progenitor cells: their role in tissue homeostasis. *Stem Cells Int*. 2016;2016:4285215.
32. Bortolotti F, Ukovich L, Razban V, et al. In vivo therapeutic potential of mesenchymal stromal cells depends on the source and the isolation procedure. *Stem Cell reports*. 2015;4: 332–339.
33. Sun K, Zhou Z, Ju X, et al. Combined transplantation of mesenchymal stem cells and endothelial progenitor cells for tissue engineering: a systematic review and meta-analysis. *Stem Cell Res Ther*. 2016;7:151.

34. Tao H, Han Z, Han ZC, Li Z. Proangiogenic features of mesenchymal stem cells and their therapeutic applications. *Stem Cells Int*. 2016;2016:1314709.
35. Bronckaers A, Hilkens P, Martens W, et al. Mesenchymal stem/stromal cells as a pharmacological and therapeutic approach to accelerate angiogenesis. *Pharmacol Ther*. 2014;143:181–196.
36. Watt SM, Gullo F, van der Garde M, et al. The angiogenic properties of mesenchymal stem/stromal cells and their therapeutic potential. *Br Med Bull*. 2013;108:25–53.
37. Oh JY, Kim MK, Shin MS, et al. The anti-inflammatory and anti-angiogenic role of mesenchymal stem cells in corneal wound healing following chemical injury. *Stem Cells*. 2008;26:1047–1055.
38. Oh JY, Roddy GW, Choi H, et al. Anti-inflammatory protein TSG-6 reduces inflammatory damage to the cornea following chemical and mechanical injury. *Proc Natl Acad Sci U S A*. 2010;107:16875–16880.
39. Clarke MR, Imhoff FM, Baird SK. Mesenchymal stem cells inhibit breast cancer cell migration and invasion through secretion of tissue inhibitor of metalloproteinase-1 and -2. *Molecular carcinogenesis*. 2015;54:1214–1219.
40. Daltro PS, Barreto BC, Silva PG, et al. Therapy with mesenchymal stromal cells or conditioned medium reverse cardiac alterations in a high-fat diet-induced obesity model. *Cytotherapy*. 2017;19:1176–1188.
41. Efimenko A, Dzhoyashvili N, Kalinina N, et al. Adipose-derived mesenchymal stromal cells from aged patients with coronary artery disease keep mesenchymal stromal cell properties but exhibit characteristics of aging and have impaired angiogenic potential. *Stem Cells Transl Med*. 2014;3:32–41.
42. Li F, Armstrong GB, Tombran-Tink J, Niyibizi C. Pigment epithelium derived factor upregulates expression of vascular endothelial growth factor by human mesenchymal stem cells: Possible role in PEDF regulated matrix mineralization. *Biochem Biophys Res Commun*. 2016;478:1106–1110.
43. Oh JY, Kim MK, Shin MS, Wee WR, Lee JH. Cytokine secretion by human mesenchymal stem cells cocultured with damaged corneal epithelial cells. *Cytokine*. 2009;46:100–103.
44. Ostanin AA, Petrovskii YL, Shevela EY, Chernykh ER. Multiplex analysis of cytokines, chemokines, growth factors, MMP-9 and TIMP-1 produced by human bone marrow, adipose tissue, and placental mesenchymal stromal cells. *Bull Exp Biol Med*. 2011;151:133–141.
45. Zolochevska O, Shearer J, Ellis J, et al. Human adipose-derived mesenchymal stromal cell pigment epithelium-derived factor cytotherapy modifies genetic and epigenetic profiles of prostate cancer cells. *Cytotherapy*. 2014;16:346–356.
46. Cappuzzello C, Doni A, Dander E, et al. Mesenchymal stromal cell-derived PTX3 promotes wound healing via fibrin remodeling. *Invest Dermatol*. 2016;136:293–300.
47. Park HW, Moon HE, Kim HS, et al. Human umbilical cord blood-derived mesenchymal stem cells improve functional recovery through thrombospondin1, pantraxin3, and vascular endothelial growth factor in the ischemic rat brain. *Neurosci Res*. 2015;93:1814–1825.
48. Kendall RL, Thomas KA. Inhibition of vascular endothelial cell growth factor activity by an endogenously encoded soluble receptor. *Proc Natl Acad Sci U S A*. 1993;90:10705–10709.
49. Cai J, Jiang WG, Grant MB, Boulton M. Pigment epithelium-derived factor inhibits angiogenesis via regulated intracellular proteolysis of vascular endothelial growth factor receptor 1. *J Biol Chem*. 2006;281:3604–3613.
50. Ambati BK, Patterson E, Jani P, et al. Soluble vascular endothelial growth factor receptor-1 contributes to the corneal antiangiogenic barrier. *Br J Ophthalmol*. 2007;91:505–508.
51. Wu FT, Stefanini MO, Mac Gabhann F, Kontos CD, Annex BH, Popel AS. A systems biology perspective on sVEGFR1: its biological function, pathogenic role and therapeutic use. *J Cell Mol Med*. 2010;14:528–552.
52. Ahmad S, Ahmed A. Elevated placental soluble vascular endothelial growth factor receptor-1 inhibits angiogenesis in preeclampsia. *Circ Res*. 2004;95:884–891.
53. Kendall RL, Wang G, Thomas KA. Identification of a natural soluble form of the vascular endothelial growth factor receptor, FLT-1, and its heterodimerization with KDR. *Biochemical Biophysical Res Communications* 1996;226:324–328.
54. Kommareddy S, Amiji M. Antiangiogenic gene therapy with systemically administered sFlt-1 plasmid DNA in engineered gelatin-based nanovectors. *Cancer Gene Ther*. 2007;14:488–498.
55. Olsson AK, Dimberg A, Kreuger J, Claesson-Welsh L. VEGF receptor signalling - in control of vascular function. *Nat Rev Mol Cell Biol*. 2006;7:359–371.
56. Kumai Y, Ooboshi H, Ibayashi S, et al. Postischemic gene transfer of soluble Flt-1 protects against brain ischemia with marked attenuation of blood-brain barrier permeability. *J Cereb Blood Flow Metab*. 2007;27:1152–1160.
57. Tsao PN, Chan FT, Wei SC, et al. Soluble vascular endothelial growth factor receptor-1 protects mice in sepsis. *Crit Care Med*. 2007;35:1955–1960.
58. Lai CM, Brankov M, Zaknich T, et al. Inhibition of angiogenesis by adenovirus-mediated sFlt-1 expression in a rat model of corneal neovascularization. *Human Gene Ther*. 2001;12:1299–1310.
59. Cho YK, Uehara H, Young JR, Archer B, Zhang X, Ambati BK. Vascular endothelial growth factor receptor 1 morpholino decreases angiogenesis in a murine corneal suture model. *Invest Ophthalmol Vis Sci*. 2012;53:685–692.
60. Kommineni VK, Nagineni CN, William A, Detrick B, Hooks JJ. IFN-gamma acts as anti-angiogenic cytokine in the human cornea by regulating the expression of VEGF-A and sVEGF-R1. *Biochem Biophys Res Commun*. 2008;374:479–484.
61. Lai CM, Shen WY, Brankov M, et al. Long-term evaluation of AAV-mediated sFlt-1 gene therapy for ocular neovascularization in mice and monkeys. *Mol Ther*. 2005;12:659–668.
62. Fitchev P, Chung C, Plunkett BA, Brendler CB, Crawford SE. PEDF & stem cells: niche vs. nurture. *Curr Drug Deliv*. 2014;11:552–560.
63. Filleur S, Nelius T, de Riese W, Kennedy RC. Characterization of PEDF: a multi-functional serpin family protein. *J Cell Biochem*. 2009;106:769–775.
64. Ek ET, Dass CR, Choong PF. PEDF: a potential molecular therapeutic target with multiple anti-cancer activities. *Trends Mol Med*. 2006;12:497–502.
65. Cai J, Wu L, Qi X, et al. PEDF regulates vascular permeability by a gamma-secretase-mediated pathway. *PLoS One*. 2011;6:e21164.
66. Zhang SX, Wang JJ, Gao G, Parke K, Ma JX. Pigment epithelium-derived factor downregulates vascular endothelial growth factor (VEGF) expression and inhibits VEGF-VEGF receptor 2 binding in diabetic retinopathy. *J Mol Endocrinol*. 2006;37:1–12.
67. Matsui T, Nishino Y, Maeda S, Yamagishi S. PEDF-derived peptide inhibits corneal angiogenesis by suppressing VEGF expression. *Microvasc Res*. 2012;84:105–108.
68. Ferrari G, Hajrasouliha AR, Sadrai Z, Ueno H, Chauhan SK, Dana R. Nerves and neovessels inhibit each other in the cornea. *Invest Ophthalmol Vis Sci*. 2013;54:813–820.
69. Karakousis PC, John SK, Behling KC, et al. Localization of pigment epithelium derived factor (PEDF) in developing and adult human ocular tissues. *Mol Vis*. 2001;7:154–163.

Investigative Ophthalmology & Visual Science

70. Ogata N, Wada M, Otsuji T, Jo N, Tombran-Tink J, Matsumura M. Expression of pigment epithelium-derived factor in normal adult rat eye and experimental choroidal neovascularization. *Invest Ophthalmol Vis Sci*. 2002;43:1168–1175.

71. Chan CK, Pham LN, Chinn C, et al. Mouse strain-dependent heterogeneity of resting limbal vasculature. *Invest Ophthalmol Vis Sci*. 2004;45:441–447.

72. Azar DT. Corneal angiogenic privilege: angiogenic and antiangiogenic factors in corneal avascularity, vasculogenesis, and wound healing (an American Ophthalmological Society thesis). *Trans Am Ophthalmol Soc*. 2006;104:264–302.

73. Dawson DW, Volpert OV, Gillis P, et al. Pigment epithelium-derived factor: a potent inhibitor of angiogenesis. *Science*. 1999;285:245–248.

74. Bouck N. PEDF: anti-angiogenic guardian of ocular function. *Trends Mol Med*. 2002;8:330–334.

75. Kim J, Escalante LE, Dollar BA, Hanson SE, Hematti P. Comparison of breast and abdominal adipose tissue mesenchymal stromal/stem cells in support of proliferation of breast cancer cells. *Cancer Invest*. 2013;31:550–554.

76. Kim J, Breunig MJ, Escalante LE, et al. Biologic and immunomodulatory properties of mesenchymal stromal cells derived from human pancreatic islets. *Cytotherapy*. 2012;14:925–935.

Investigative Ophthalmology & Visual Science